Supporting Information

Activating Titanium Dioxide as a New Efficient Electrocatalyst: From Theory to Experiment

Bowen Ren,[†] *Qiuyan Jin,*[†] *Yinwei Li,*[‡] *Yan Li,*[†]* *Hao Cui*[†]* *and Chengxin Wang*[†]*

[†]State Key Laboratory of Optoelectronic Materials and Technologies, School of Materials Science and Engineering, The Key Laboratory of Low-Carbon Chemistry & Energy Conservation of Guangdong Province, Sun Yat-sen University, Guangzhou 510275, China.

[‡]School of Physics and Electronic Engineering, Jiangsu Normal University, Xuzhou 221116, China

*Corresponding author: Fax: +86-20-8411-3901; E-mail: liyan266@mail.sysu.edu.cn; cuihao3@mail.sysu.edu.cn; wchengx@mail.sysu.edu.cn;

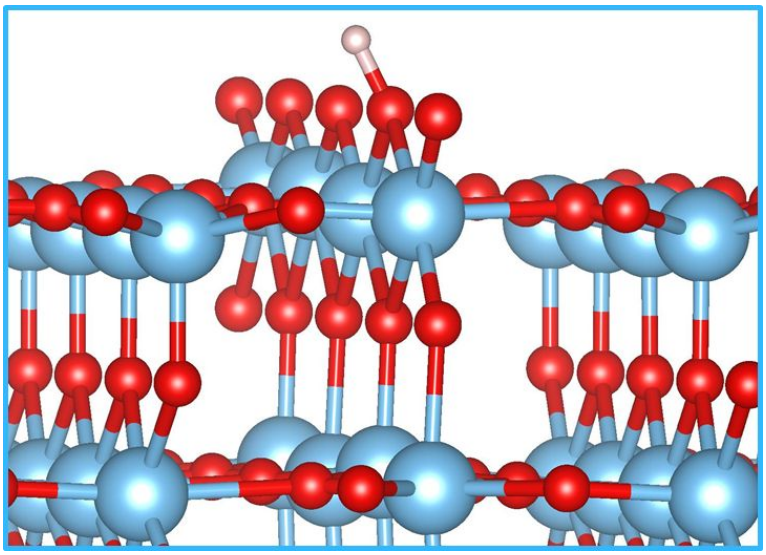

Figure S1. Schematic models with H* adsorbed on the surfaces of R-TiO_2. Color code: Ti: blue; O: red; H*: white.

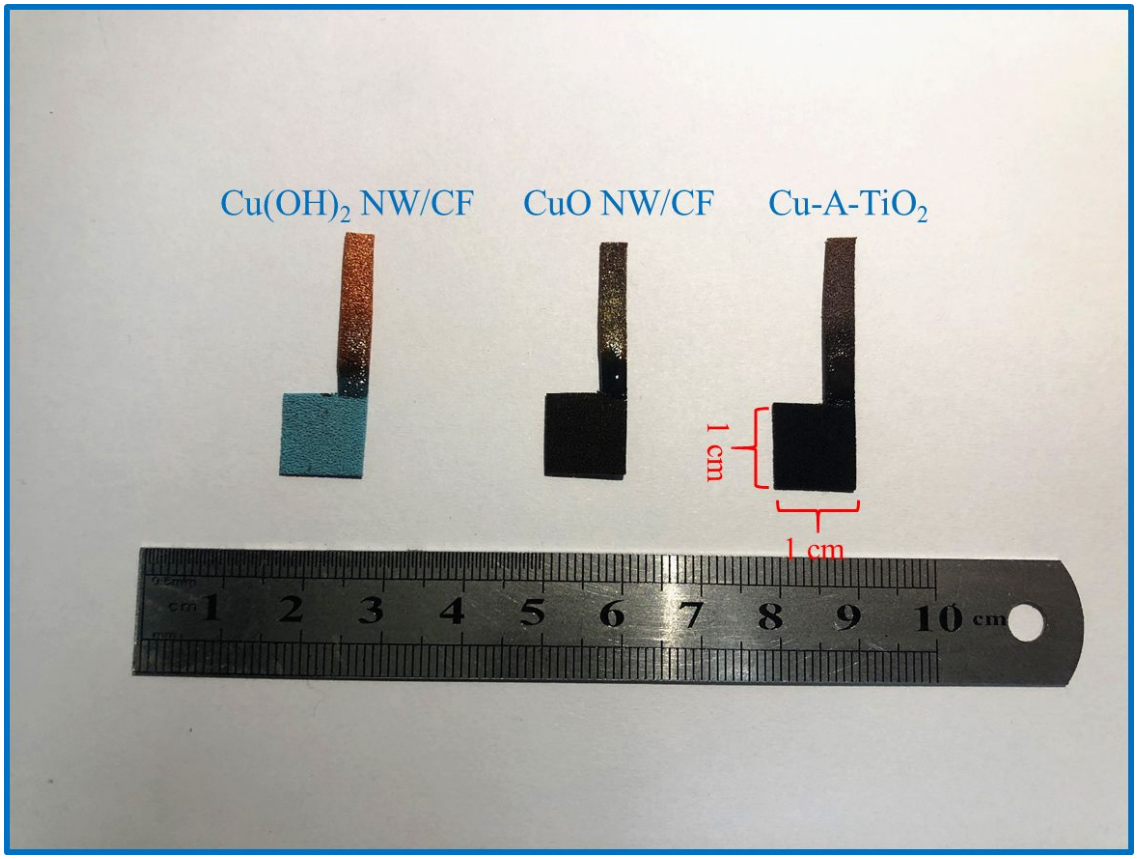

Figure S2. Optical photograph of bare $Cu(OH)_2$ NW/CF (left), CuO NW/CF (middle), and Cu-A-TiO_2 (right).

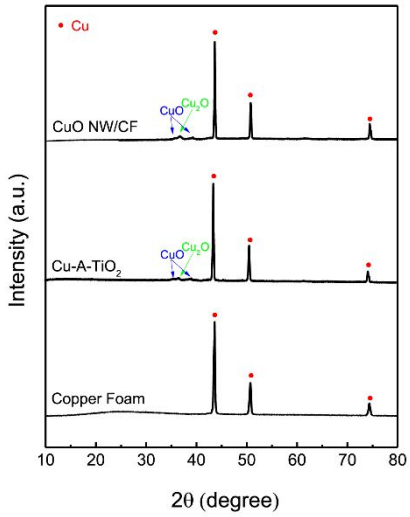

Figure S3. XRD patterns of CuO NW/CF, Cu-A-TiO_2 and copper foam. There is no changes in XRD diffraction peak could be observed after TiO_2 deposition.

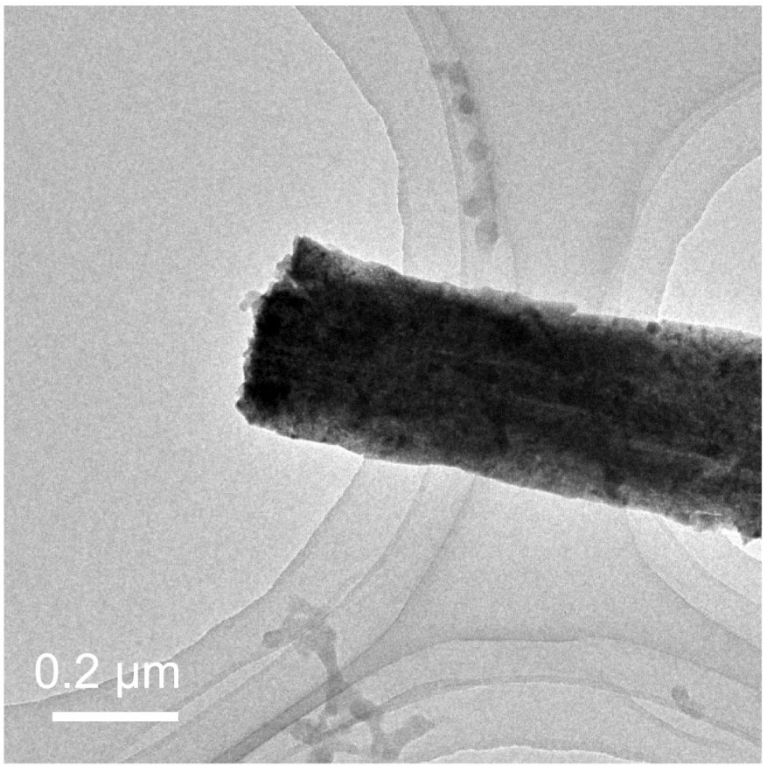

Figure S4. TEM image of CuO NW/CF.

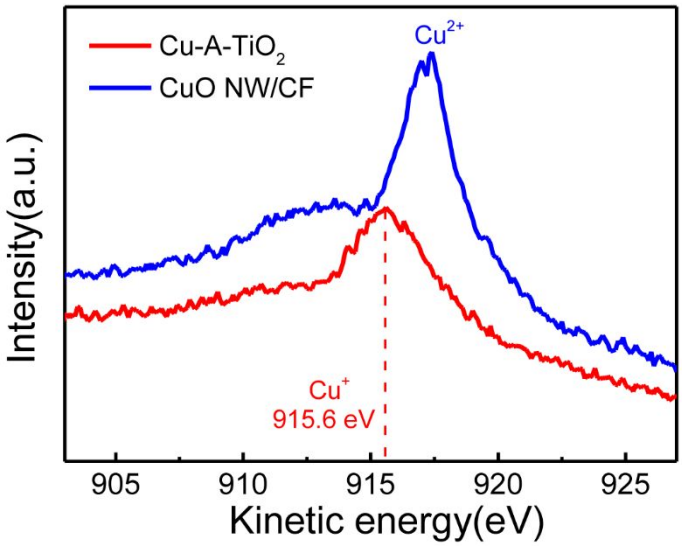

Figure S5. Cu LMM Auger spectra for CuO NW/CF and Cu-A-TiO_2.

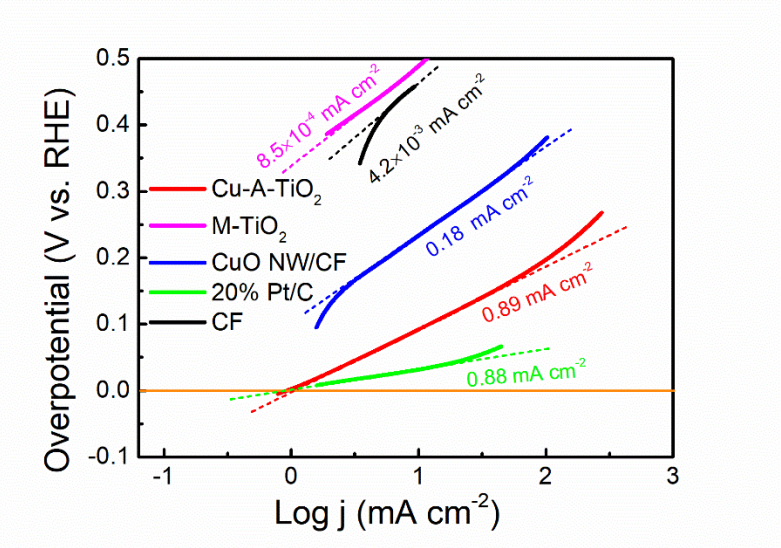

Figure S6. Exchange current densities for as-synthesized catalysts in 1 M KOH for HER, which were calculated from Tafel plots by extrapolation method.

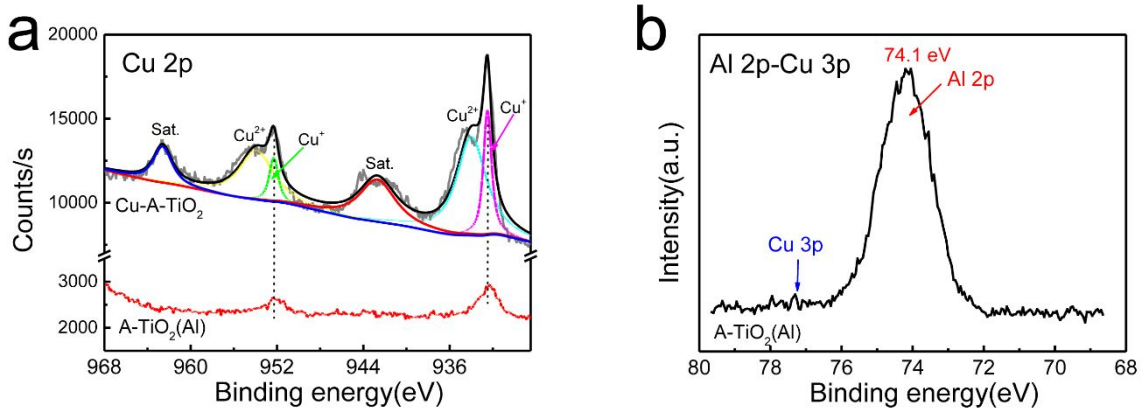

Figure S7. a) Cu 2p spectra of Cu-A-TiO_2 and A-TiO_2(Al). b) Cu 3p-Al 2p spectra of A-TiO_2(Al).

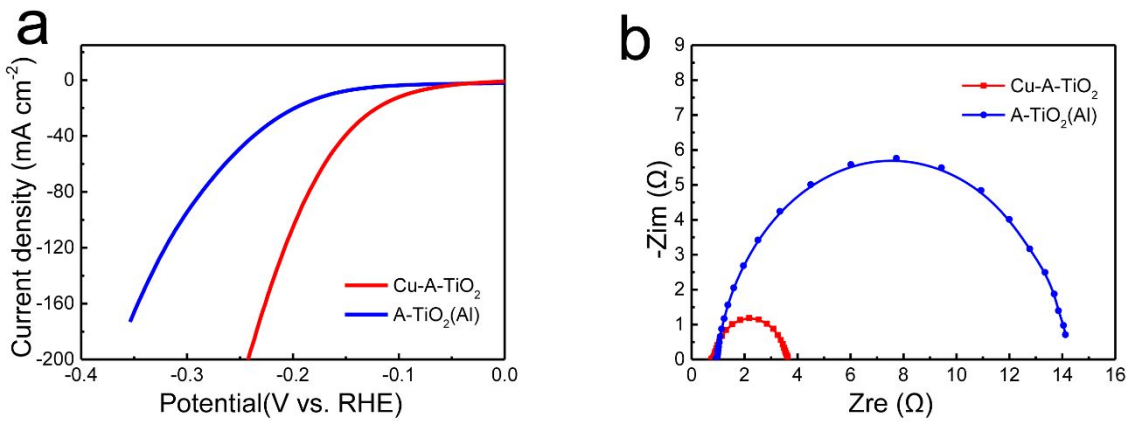

Figure S8. a) iR-corrected polarization curves of Cu-A-TiO_2 and A-TiO_2(Al) at 2 mV s^{-1} in 1 M KOH. b) Electrochemical impedance spectra of Cu-A-TiO_2 and A-TiO_2(Al) with overpotential of 150 mV.

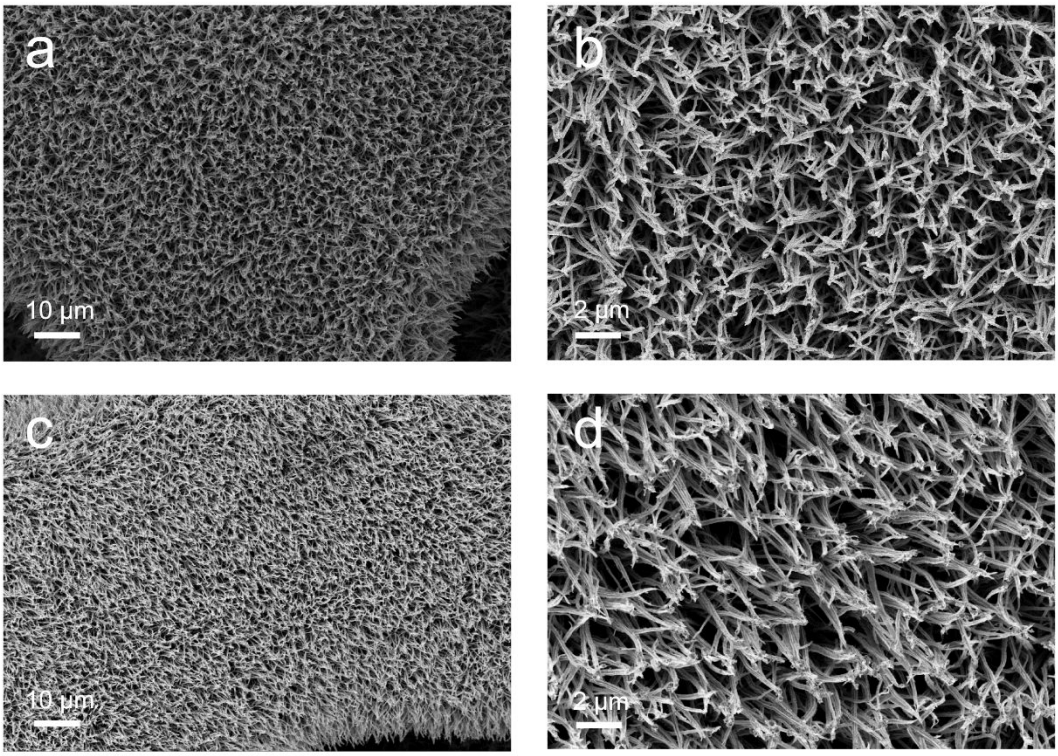

Figure S9. SEM images of Cu-A-TiO_2 after long-term durability test in a,b) 1 M KOH and c,d) 1 M PBS.

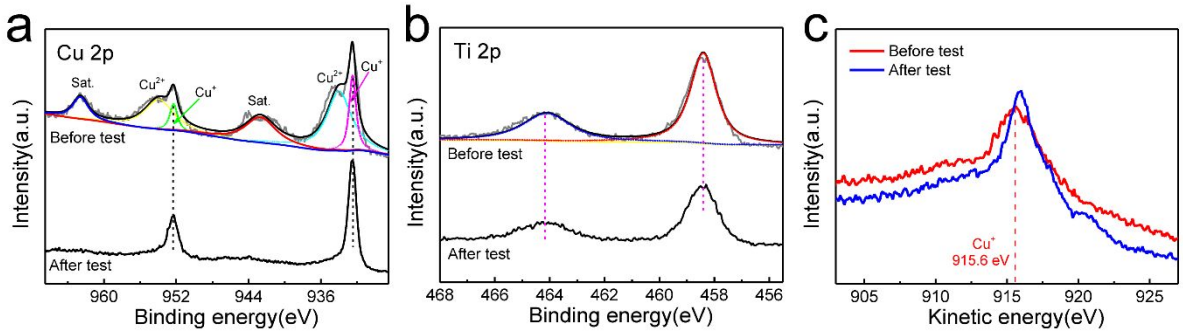

Figure S10. XPS Spectra of Cu-A-TiO_2 composite after HER stability test. a) Cu 2p, b) Ti 2p, and c) Cu LMM.

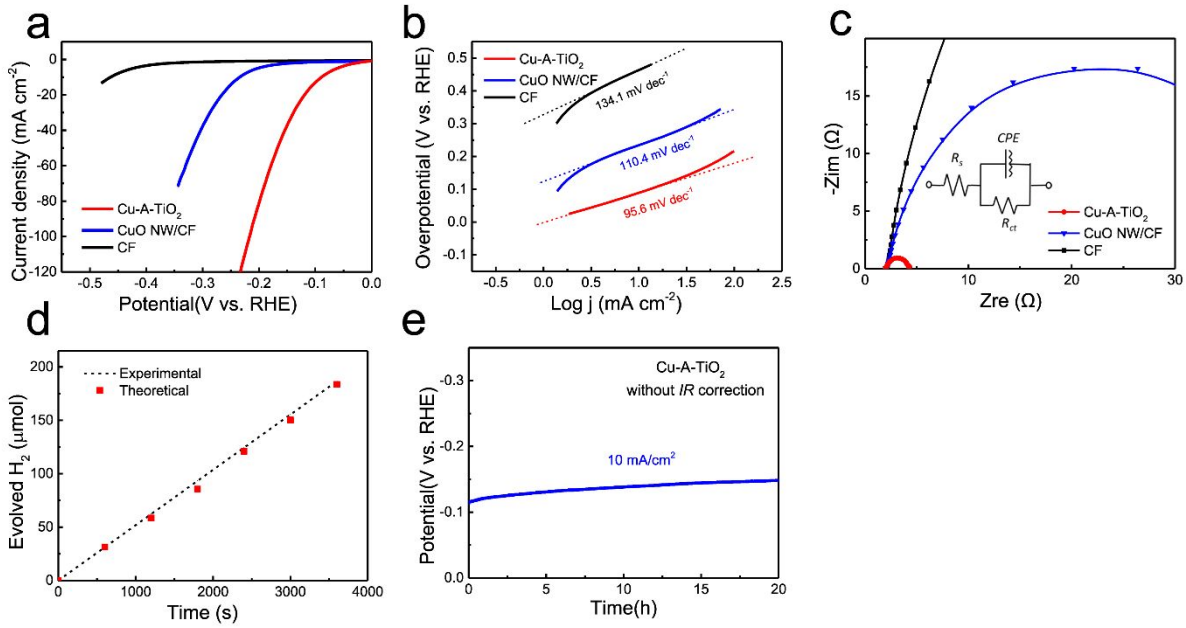

Figure S11. Electrochemical tests in 1 M PBS solution. (a) Polarization curves and (b) Tafel plots of Cu-A-TiO_2 in comparison with CuO NW/CF and CF. (c) The Nyquist plots with overpotential of 150 mV. The inset in (c) shows corresponding equivalent circuit model. (d) The comparison of the experimentally quantified H_2 amount gas with theoretically calculated gas for Cu-A-TiO_2 at 10 mA cm^{-2}. (e) Stability testing of Cu-A-TiO_2 by chronopotentiometry at a static current density of 10 mA cm^{-2}.

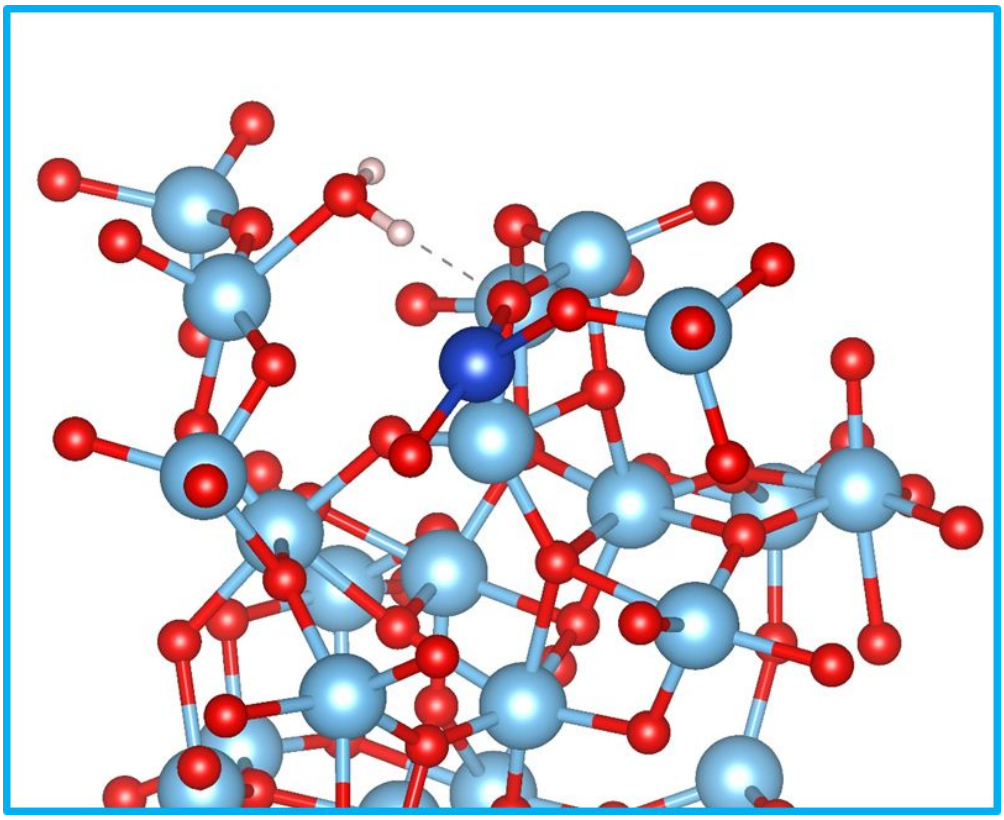

Figure S12. Schematic models with H_2O molecule adsorbed on the surface of Cu-A-TiO_2. The dotted line shows the hydrogen bond between the H_2O molecule and the surface oxygen atom.

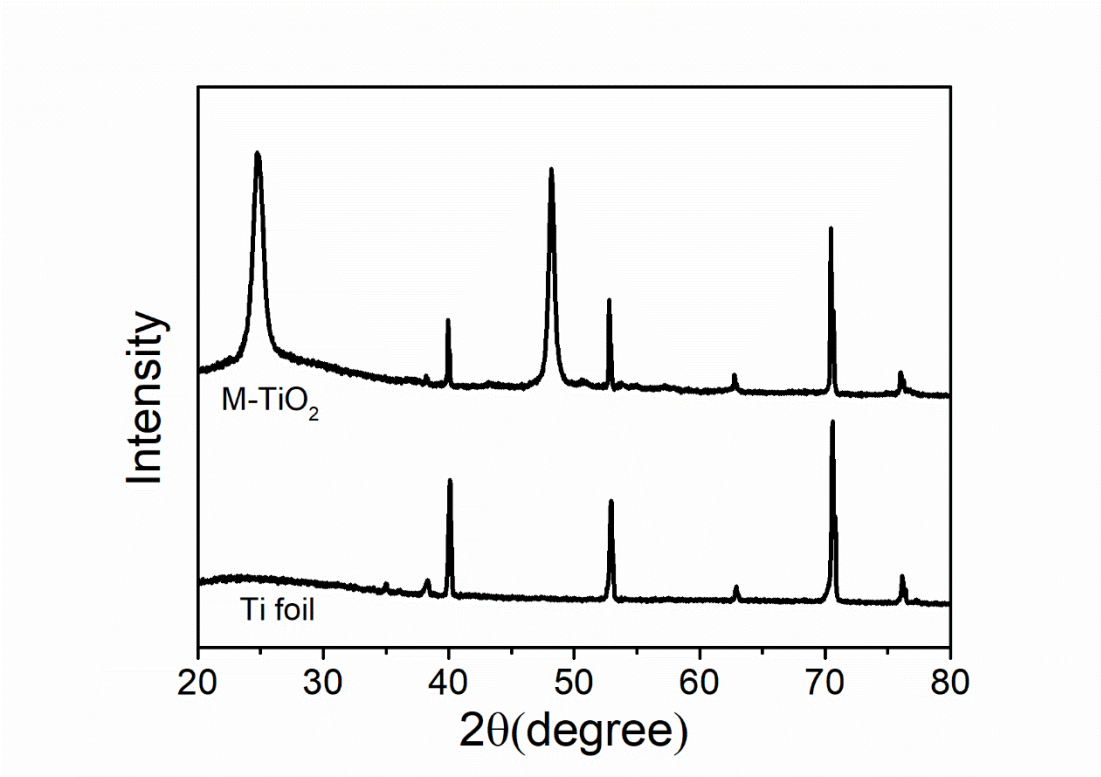

Figure S13. XRD patterns of M-TiO_2 and Ti foil.

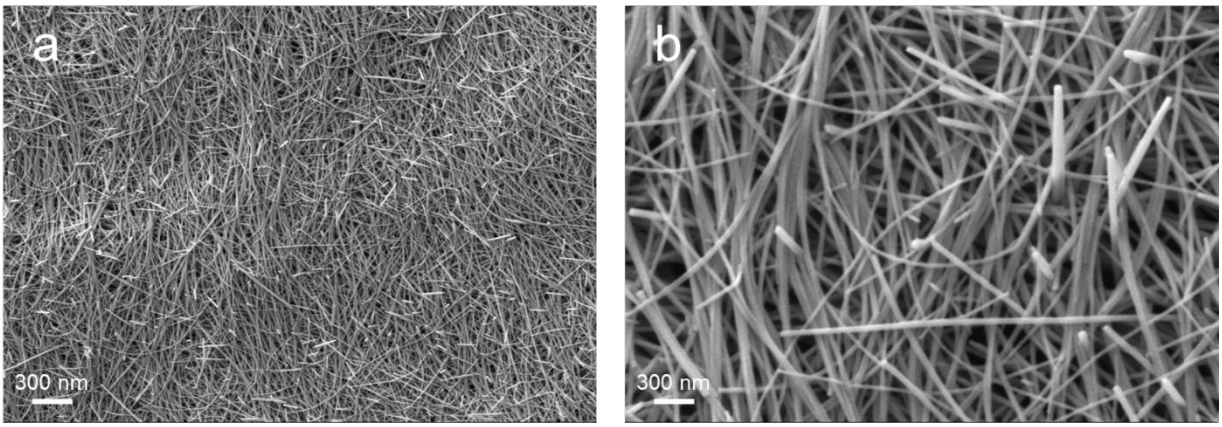

Figure S14. a) Low- and b) high-magnification SEM images of M-TiO_2.

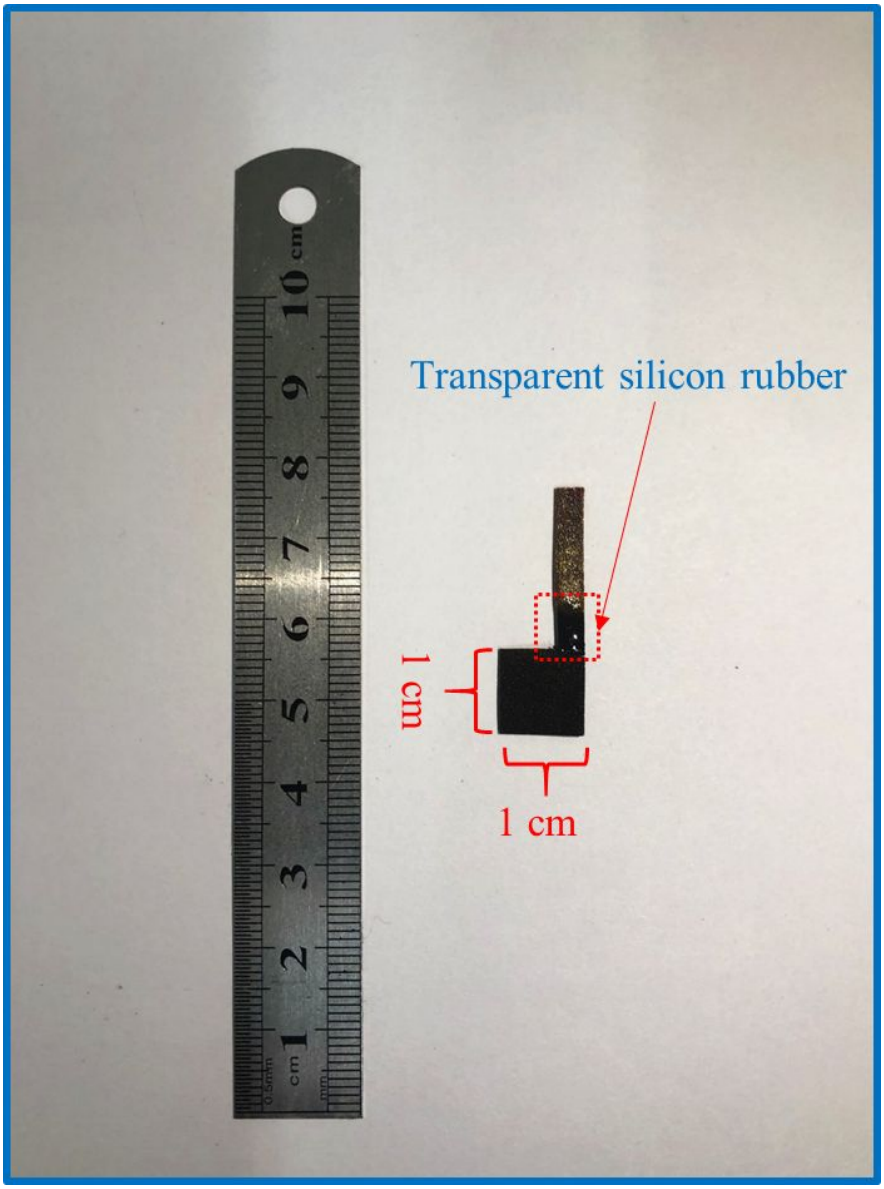

Figure S15. Optical photograph of preparation for the working electrode. The as-synthesized sample with copper foam was cut into a specific shape. And electrochemically inert silicon rubber was used to precisely define an active geometric area.

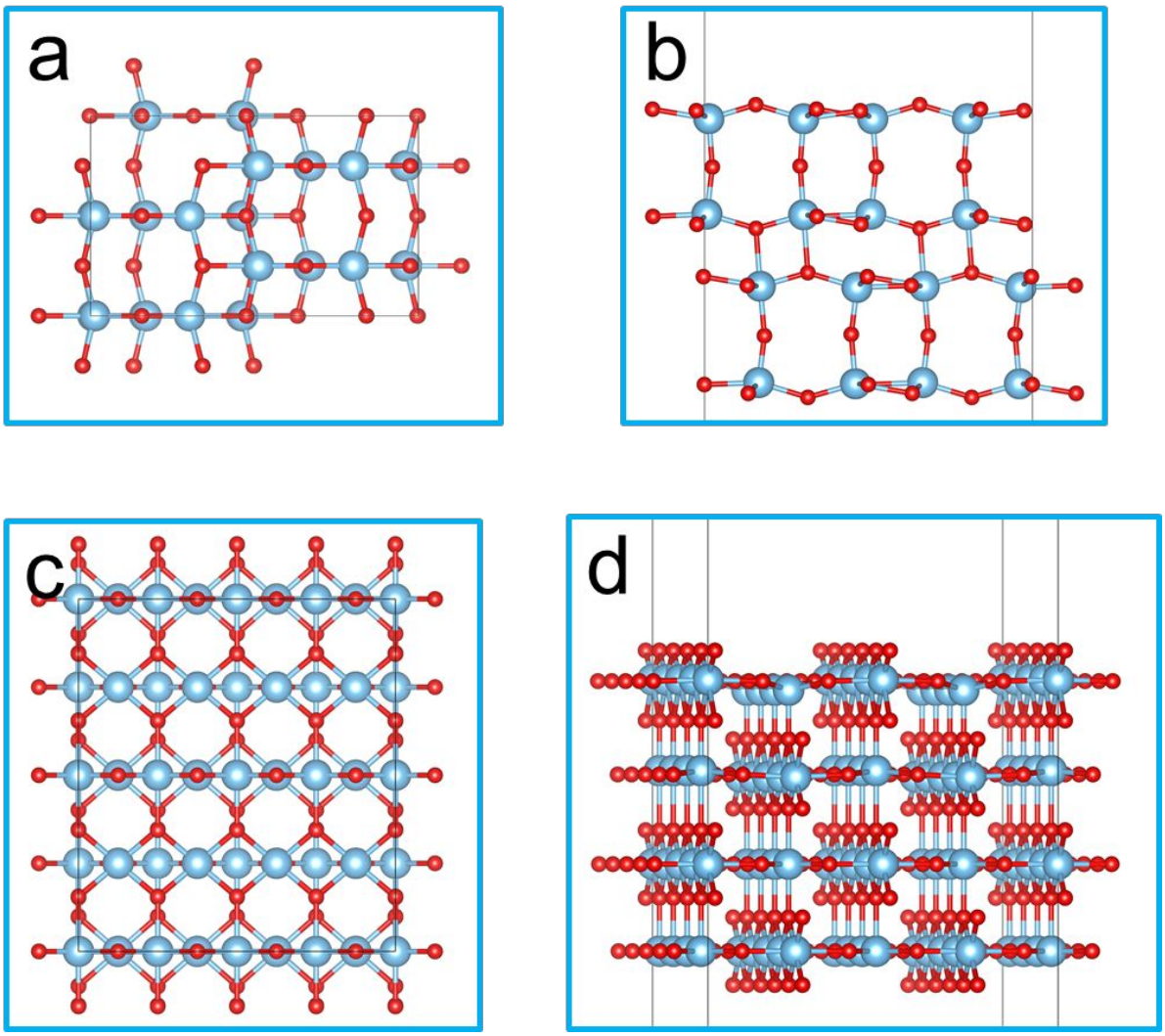

Figure S16. Schematic models of a,b) M-TiO_2 and c,d) R-TiO_2. Color code: Ti: blue; O: red.

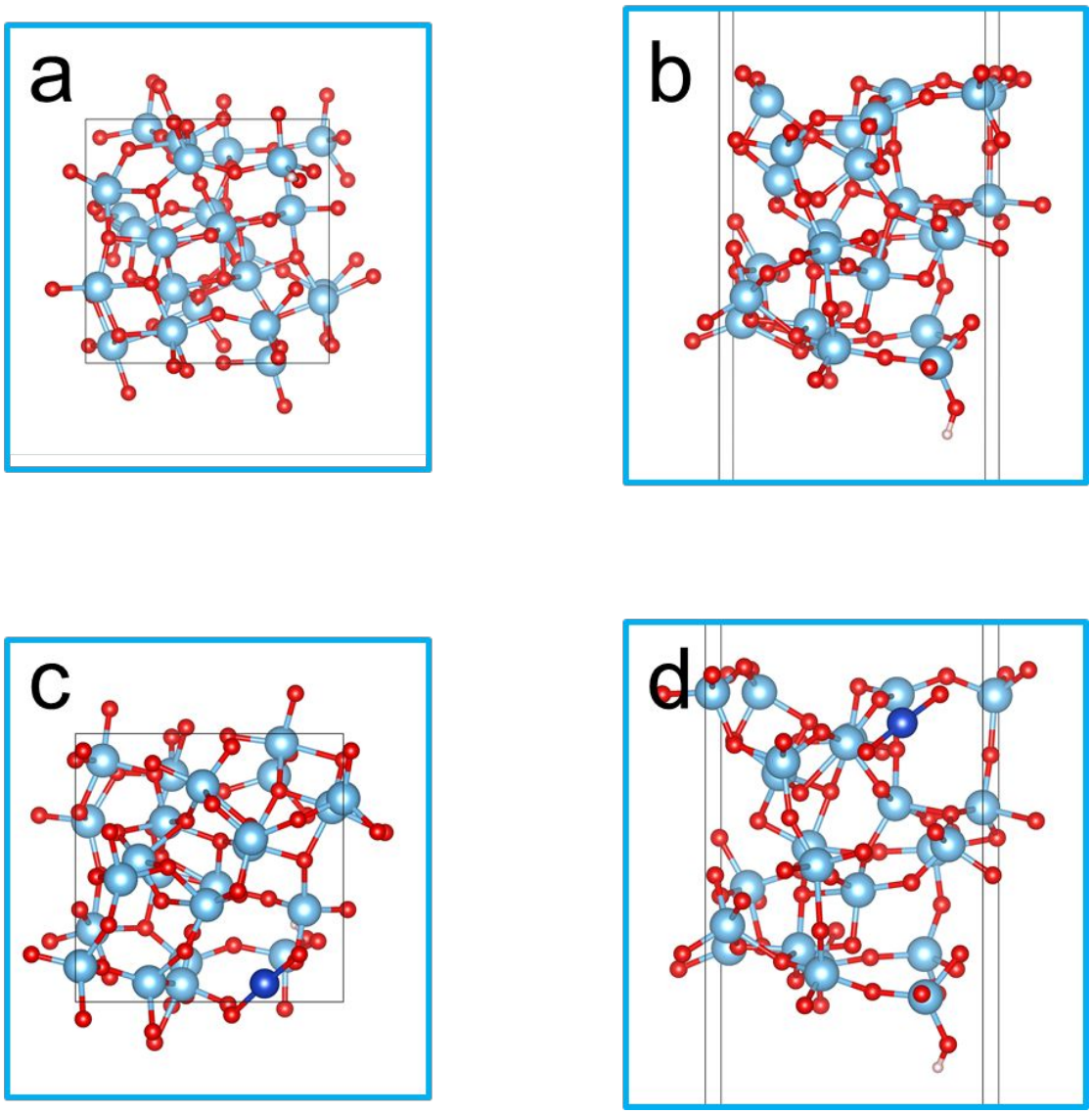

Figure S17. Schematic models of a,b) A-TiO_2 and c,d) Cu-A-TiO_2. Color code: Ti: blue; O: red; Cu: dark blue.

Table S1. Comparisons of HER performance of Cu-A-TiO_2 with other reported non-noble-metal catalysts.

Electrocatalysts	Electrolyte	Overpotential at 10 mA cm^{-2} (mV)	Tafel solpe (mV dec^{-1})	Ref.
Cu-A-TiO_2	1 M KOH	92	96	This work
OV-high TiO_2	1 M KOH	~600	187.5	1
$TiO_{1.23}$	0.5 M H_2SO_4	198	88	2
CFP–FeP HNA	1 M KOH	181	134	3
Fe–O–P NRs	1 M KOH	110	128	4
Cu@NiFe LDH	1 M KOH	116	58.9	5
Co_3O_4@Ni	1 M KOH	130	53	6
CoS_2	1 M KOH	193	88	7
NiCoP/CC	1 M KOH	62	68	8
O,Cu−CoP	1 M KOH	72	62	9
$MoNi_4$	1 M KOH	15	30	10
NiS_2-MoS_2	1 M KOH	204	65	11
Ni_2P-Ni_3S_2 HNAs/NF	1 M KOH	80	65	12
porous MoO_2	1 M KOH	27	41	13
$Co_2Mo_3O_8$/Co/NF	1 M KOH	50	49	14
N doped Mo_2C nanosheets	1 M KOH	140	65	15
WO_2 HN/NF	1 M KOH	48	43	16

Table S2. Mean value (standard deviation) of the electrochemical HER kinetic parameters of tested cathode.

Tested cathode	Overpotential at j =10 mA cm^{-2} (mV)	Tafel slope (mV dec^{-1})	j_0 (mA cm^{-2})
Cu-A-TiO_2	90(2.08)	94(1.52)	0.92(0.11)
20% Pt/C	33(0.57)	31(1.15)	0.88(0.007)
M-TiO_2	>400	163(3.06)	8.4(0.4)×10^{-4}
CuO NW/CF	236(2.65)	135(1.50)	0.19(0.04)
CF	>400	169(2.33)	4.2(0.25)×10^{-3}

Table S3. Bandgaps (eV) of TiO_2 (rutile and monoclinic phases).

	Rutile	Monoclinic
Our simulations	2.23	3.11
Other simulations	2.28[17]	3.22[17]
Experiment	3.03[18]	3.20[19]

Table S4. Adsorption energies (eV) of H_2O and H on TiO_2 (rutile and monoclinic phases).

	H_2O		H	
	Rutile	Monoclinic	Rutile	Monoclinic
Our simulations	-0.91	-0.47	-0.42	0.04
Other simulations	-0.93[20]	-0.46[21]	-0.55[20]	N/A

Table S5. Adsorption free energies (eV) of H_2O and H on TiO_2 (rutile and monoclinic phases).

	H_2O		H	
	Rutile	Monoclinic	Rutile	Monoclinic
Our simulations	-0.25	0.19	-0.18	0.28

References

(1) Feng, H.; Xu, Z.; Ren, L.; Liu, C.; Zhuang, J.; Hu, Z.; Xu, X.; Chen, J.; Wang, J.; Hao, W.; Du, Y.; Dou, S. Activating Titania for Efficient Electrocatalysis by Vacancy Engineering. ACS Catal. 2018, 8 (5), 4288–4293. https://doi.org/10.1021/acscatal.8b00719.

(2) Swaminathan, J.; Subbiah, R.; Singaram, V. Defect-Rich Metallic Titania ($TiO_{1.23}$)—An Efficient Hydrogen Evolution Catalyst for Electrochemical Water Splitting. *ACS Catal.* **2016**, *6* (4), 2222–2229. https://doi.org/10.1021/acscatal.5b02614.

(3) Lv, C.; Peng, Z.; Zhao, Y.; Huang, Z.; Zhang, C. The Hierarchical Nanowires Array of Iron Phosphide Integrated on a Carbon Fiber Paper as an Effective Electrocatalyst for Hydrogen Generation. *J Mater Chem A* **2016**, *4* (4), 1454–1460. https://doi.org/10.1039/C5TA08715E.

(4) Huang, J.; Su, Y.; Zhang, Y.; Wu, W.; Wu, C.; Sun, Y.; Lu, R.; Zou, G.; Li, Y.; Xiong, J. FeOx/FeP Hybrid Nanorods Neutral Hydrogen Evolution Electrocatalysis: Insight into Interface. *J. Mater. Chem. A* **2018**, *6* (20), 9467–9472. https://doi.org/10.1039/C8TA02204F.

(5) Yu, L.; Zhou, H.; Sun, J.; Qin, F.; Yu, F.; Bao, J.; Yu, Y.; Chen, S.; Ren, Z. Cu Nanowires Shelled with NiFe Layered Double Hydroxide Nanosheets as Bifunctional Electrocatalysts for Overall Water Splitting. *Energy Environ. Sci.* **2017**, *10* (8), 1820–1827. https://doi.org/10.1039/C7EE01571B.

(6) Li, R.; Zhou, D.; Luo, J.; Xu, W.; Li, J.; Li, S.; Cheng, P.; Yuan, D. The Urchin-like Sphere Arrays Co_3O_4 as a Bifunctional Catalyst for Hydrogen Evolution Reaction and Oxygen Evolution Reaction. *J. Power Sources* **2017**, *341*, 250–256. https://doi.org/10.1016/j.jpowsour.2016.10.096.

(7) Guan, C.; Liu, X.; Elshahawy, A. M.; Zhang, H.; Wu, H.; Pennycook, S. J.; Wang, J. Metal–Organic Framework Derived Hollow CoS_2 Nanotube Arrays: An Efficient Bifunctional Electrocatalyst for Overall Water Splitting. *Nanoscale Horiz.* **2017**, *2* (6), 342–348. https://doi.org/10.1039/C7NH00079K.

(8) Du, C.; Yang, L.; Yang, F.; Cheng, G.; Luo, W. Nest-like NiCoP for Highly Efficient Overall Water Splitting. *ACS Catal.* **2017**, *7* (6), 4131–4137. https://doi.org/10.1021/acscatal.7b00662.

(9) Xu, K.; Sun, Y.; Sun, Y.; Zhang, Y.; Jia, G.; Zhang, Q.; Gu, L.; Li, S.; Li, Y.; Fan, H. J. Yin-Yang Harmony: Metal and Nonmetal Dual-Doping Boosts Electrocatalytic Activity for Alkaline Hydrogen Evolution. *ACS Energy Lett.* **2018**, *3* (11), 2750–2756. https://doi.org/10.1021/acsenergylett.8b01893.

(10) Zhang, J.; Wang, T.; Liu, P.; Liao, Z.; Liu, S.; Zhuang, X.; Chen, M.; Zschech, E.; Feng, X. Efficient Hydrogen Production on $MoNi_4$ Electrocatalysts with Fast Water Dissociation Kinetics. *Nat. Commun.* **2017**, *8*, 15437. https://doi.org/10.1038/ncomms15437.

(11) Kuang, P.; Tong, T.; Fan, K.; Yu, J. In Situ Fabrication of Ni–Mo Bimetal Sulfide Hybrid as an Efficient Electrocatalyst for Hydrogen Evolution over a Wide PH Range. *ACS Catal.* **2017**, *7* (9), 6179–6187. https://doi.org/10.1021/acscatal.7b02225.

(12) Zeng, L.; Sun, K.; Wang, X.; Liu, Y.; Pan, Y.; Liu, Z.; Cao, D.; Song, Y.; Liu, S.; Liu, C. Three-Dimensional-Networked Ni_2P/Ni_3S_2 Heteronanoflake Arrays for Highly Enhanced Electrochemical Overall-Water-Splitting Activity. *Nano Energy* **2018**, *51*, 26–36. https://doi.org/10.1016/j.nanoen.2018.06.048.

(13) Jin, Y.; Wang, H.; Li, J.; Yue, X.; Han, Y.; Shen, P. K.; Cui, Y. Porous MoO_2 Nanosheets as Non-Noble Bifunctional Electrocatalysts for Overall Water Splitting. *Adv. Mater.* **2016**, *28* (19), 3785–3790. https://doi.org/10.1002/adma.201506314.

(14) Ou, Y.; Tian, W.; Liu, L.; Zhang, Y.; Xiao, P. Bimetallic $Co_2Mo_3O_8$ Suboxides Coupled with Conductive Cobalt Nanowires for Efficient and Durable Hydrogen Evolution in Alkaline Electrolyte. *J. Mater. Chem. A* **2018**, *6* (12), 5217–5228. https://doi.org/10.1039/C7TA11401J.
(15) Jia, J.; Xiong, T.; Zhao, L.; Wang, F.; Liu, H.; Hu, R.; Zhou, J.; Zhou, W.; Chen, S. Ultrathin N-Doped Mo_2C Nanosheets with Exposed Active Sites as Efficient Electrocatalyst for Hydrogen Evolution Reactions. *ACS Nano* **2017**, *11* (12), 12509–12518. https://doi.org/10.1021/acsnano.7b06607.
(16) Shu, C.; Kang, S.; Jin, Y.; Yue, X.; Shen, P. K. Bifunctional Porous Non-Precious Metal WO_2 Hexahedral Networks as an Electrocatalyst for Full Water Splitting. *J. Mater. Chem. A* **2017**, *5* (20), 9655–9660. https://doi.org/10.1039/C7TA01527E.
(17) German, E.; Faccio, R.; Mombrú, A. W. A DFT + U Study on Structural, Electronic, Vibrational and Thermodynamic Properties of TiO_2 Polymorphs and Hydrogen Titanate: Tuning the Hubbard 'U-Term.' *J. Phys. Commun.* **2017**, *1* (5), 055006. https://doi.org/10.1088/2399-6528/aa8573.
(18) Amtout, A.; Leonelli, R. Optical Properties of Rutile near Its Fundamental Band Gap. *Phys Rev B* **1995**, *51* (11), 6842–6851. https://doi.org/10.1103/PhysRevB.51.6842.
(19) Tang, H.; Berger, H.; Schmid, P. E.; Lévy, F.; Burri, G. Photoluminescence in TiO_2 Anatase Single Crystals. *Solid State Commun.* **1993**, *87* (9), 847–850. https://doi.org/10.1016/0038-1098(93)90427-O.
(20) Kowalski, P. M.; Meyer, B.; Marx, D. Composition, Structure, and Stability of the Rutile TiO_2 Surface: Oxygen Depletion, Hydroxylation, Hydrogen Migration, and Water Adsorption. *Phys Rev B* **2009**, *79* (11), 115410. https://doi.org/10.1103/PhysRevB.79.115410.
(21) Vittadini, A.; Casarin, M.; Selloni, A. Hydroxylation of TiO_2-B: Insights from Density Functional Calculations. *J. Mater. Chem.* **2010**, *20* (28), 5871–5877. https://doi.org/10.1039/C0JM00422G.